# Studies in nitrosopyrazoles. Part 2.[1] Solution and solid-state NMR studies of 3,5-disubstituted and 1,3,5-trisubstituted-4-nitrosopyrazoles. Crystal structures of 1,3,5-trimethyl-4-nitrosopyrazole and 3,5-di-*tert*-butyl-4-nitrosopyrazole

**Daniel A. Fletcher,[a] Brian G. Gowenlock,[a] Keith G. Orrell,[a] Vladimir Šik,[a] David E. Hibbs,[b] Michael B. Hursthouse[b] and K. M. Abdul Malik[b]**

[a] *Department of Chemistry, The University, Exeter, UK EX4 4QD*
[b] *Department of Chemistry, University of Wales Cardiff, PO Box 912, Cardiff, UK CF1 3TB*

**Variable temperature NMR studies of a range of 3,5-disubstituted (R = R′ = Me, Bu$^t$) and 1,3,5-trisubstituted (R, R′, R″ = Me, $CF_3$, Ph or Bu$^i$)-4-nitrosopyrazoles have led to the identification of individual rotational isomers at low solution temperatures arising from the slowing down of the rotation of the nitroso function with respect to the pyrazole ring. Rotational energy barriers [$\Delta G^{\ddagger}$ (298.15 K)], calculated by total NMR bandshape analysis, were in the range 38–65 kJ mol$^{-1}$. The −N=O rotation process also occurs in the solid state and leads to disorder in the crystal structures of 1,3,5-trimethyl-4-nitrosopyrazole and 3,5-di-*tert*-butyl-4-nitrosopyrazole. The 1-*H*-3,5-disubstituted-4-nitrosopyrazoles exhibit rapid annular tautomerism in solution.**

4-Nitrosopyrazoles have been known for nearly a century,[2] yet there has been no detailed study made of their solid state and solution structures. The earlier part[1] of this work described preparative routes to a number of 3,5-disubstituted and 1,3,5-trisubstituted-4-nitrosopyrazoles and presented characterisation data (*viz*. elemental analyses, mass spectral data, room temperature $^{13}$C and $^1$H NMR data, visible absorption data and dipole moments) for these compounds. This present paper examines more closely the structural features of these, and other, substituted 4-nitrosopyrazoles, using particularly dynamic NMR techniques.[3] Variable temperature NMR can provide much insight into the restricted rotation of nitroso groups, *e.g.* in *C*-nitrosobenzene systems.[4] This arises from the exceptionally high degree of chemical shielding anisotropy associated with the −N=O group,[5,6] which leads to very extensive changes in NMR spectra of *C*-nitroso compounds when recorded at different temperatures.

The compounds investigated here fall into two classes, namely N−H and *N*-alkyl/aryl compounds. In the N−R compounds the 3- and 5-substituents may be the same (R′ = R″) or different (R′ ≠ R″). In the latter case, two chemically distinct isomers may arise from the standard preparative route, namely nitrosation of a β-diketone to give the oxime followed by condensation with a monosubstituted hydrazine.[7–12] Both structural isomers were isolated when R′, R″ = Me, Bu$^i$ (compounds **7**, **8**) and when R′, R″ = Me, $CF_3$ (**9**, **10**), but only a single isomer obtained when R′, R″ = Ph, Me (**6**). These pairs of isomers were unambiguously identified by NMR spectroscopy. In the N−H compounds only symmetrical substitution at the 3- and 5-positions (R′ = R″) was examined (compounds **1** and **2**) and thus only a single structural isomer is possible. Rapid tautomeric equilibria of the N−H function[13] causes these structures to have effective $C_{2v}$ symmetry at ambient temperatures where the −N=O rotation is also fast on the NMR timescale.

This paper examines in some detail the temperature dependence of the nitroso group rotation in 10 substituted 4-nitrosopyrazoles and presents crystal structures for two of them (**2**, **3**).


| | R | R′ |
|---|---|---|
| 1 | Me | Me |
| 2 | Bu$^t$ | Bu$^t$ |

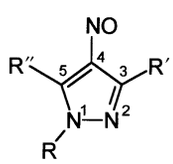


| | R | R′ | R″ |
|---|---|---|---|
| 3 | Me | Me | Me |
| 4 | Ph | Me | Me |
| 5 | Me | Bu$^t$ | Bu$^t$ |
| 6 | Me | Ph | Me |
| 7 | Me | Me | Bu$^i$ |
| 8 | Me | Bu$^i$ | Me |
| 9 | Me | Me | $CF_3$ |
| 10 | Me | $CF_3$ | Me |

## Experimental

### Instrumental

**Physical methods.** All variable temperature solution state NMR spectra were recorded on Bruker AM250, Bruker AC300 or Bruker Avance DRX 400 spectrometers each equipped with a standard B-VT 1000 variable temperature unit. The $^1$H spectra were recorded at 250.13, 300.13 and 400.13 MHz respectively, $^{13}$C spectra at 62.90, 75.47 and 100.62 MHz and $^{19}$F spectra at 235.32, 282.36 and 376.44 MHz. The $^1$H and $^{13}$C

shifts are relative to $SiMe_4$; $^{19}F$ shifts are relative to $C_6F_6$. NMR probe temperatures, based on calibration against a Comark digital thermometer, are accurate to *ca.* ±1 °C. Spectra were recorded as solutions in $CDCl_3$ or $CD_2Cl_2$ unless stated otherwise. NMR bandshapes were analysed using the authors' version of the DNMR3 program.[14] The computer simulated spectra were compared visually with those experimentally obtained and the 'best fit' rate constants used to calculate the activation parameters, from a least squares fitting of the Eyring plot, using the THERMO program.[15] The errors quoted are based on the goodness-of-fit of this plot. The 2-dimensional EXSY spectra were obtained using the Bruker automation program NOESYPH. The sizes of the frequency domains, *F*1 and *F*2 were 512 words. Data processing incorporated an exponential window function with a line broadening of 0.5 Hz in both frequency dimensions. Intensities of diagonal and cross peaks were measured accurately by integrating spectral rows. Rate data were calculated from these signal intensities using the D2DNMR program.[16]

Solid state $^{13}C$ CP/MAS spectra were recorded at 75.42 MHz on a Varian VXR-300 spectrometer at the University of Durham Industrial Research Laboratories. The non-quaternary suppression (NQS) technique[17] was applied to the room temperature spectra and, in some cases, total sideband suppression (TOSS)[18] was applied. For all spectra the following conditions were used, acquisition time 203 ms, relaxation delay 30.0 s, CP contact time 5 ms. Gaussian broadening of 0.008 s was applied to all spectral lines.

IR spectra were recorded as a pressed disc (KBr) or liquid film (NaCl plate) on a Nicolet Magna FTIR spectrometer equipped with a CsI beamsplitter, operating in the range 4000–200 $cm^{-1}$. UV–VIS spectra were recorded as solutions on a Philips PU 9720 scanning spectrometer. Electron-impact mass spectra were obtained on a Kratos Profile spectrometer with an electron beam energy of 70 eV and a probe temperature of 150 °C. The elemental analysis was carried out at Butterworth Laboratories Ltd., Teddington, Middlesex.

**Compounds.** The substituted 4-nitrosopyrazoles, compounds **1**–**8**, were prepared as previously.[1] The yield of **5** was improved over the previous report[1] by using 1 equiv. of methylhydrazine rather than an excess. Compounds **7** and **8** were prepared as reported[1] but separation of these isomers by column chromatography was more complete using diethyl ether instead of diethyl ether–toluene as eluent. Compounds **9** and **10** were prepared as follows.

1,3-*Dimethyl*-5-*trifluoromethyl*-4-*nitrosopyrazole* (**9**) *and* 1,5-*dimethyl*-3-*trifluoromethyl*-4-*nitrosopyrazole* (**10**).—1,1,1-Trifluoroheptane-2,4-dione (1.54 g, 0.01 mol) was added to concentrated hydrochloric acid (0.9 $cm^3$) and water (5 $cm^3$). This mixture was cooled in ice and sodium nitrite (0.71 g, 0.01 mol), dissolved in water (2 $cm^3$), was added very slowly dropwise. The solution was placed in the fridge (2 °C) overnight until the orange colour of the oil had disappeared. Methylhydrazine (0.461 g, 0.01 mol) was added to the solution with stirring. The colour of the solution went from yellow through green to blue followed by the formation of a blue oil. This oil was separated and dissolved in light petroleum, bp 40–60 °C (4 $cm^3$), and then placed in the freezer overnight. Blue crystals of 1,5-dimethyl-3-trifluoromethyl-4-nitrosopyrazole had formed and were separated by filtration and recrystallised again from light petroleum, bp 40–60 °C. The remaining solution was taken and the solvent evaporated to yield the other isomer as a thick, blue oil. 1,5-*Dimethyl*-3-*trifluoromethyl*-4-*nitrosopyrazole*, mp 41–42 °C. $\nu_{max}$(KBr)/$cm^{-1}$ 1506, 1497, 1460, 1400, 1380, 1294, 1265, 1178, 1142, 1111, 1016, 792, 723, 446; $\lambda_{max}(CH_2Cl_2)$/nm 701; *m*/*z* 193 [$M^+$, 9.3%], 177 [7.2%], 149 [32.2%], 85 [33.8%], 69 [61.6%], 57 [100.0%]; elemental analysis, calc. C 37.33% (Found 37.32%), H 3.09% (3.13%), N 21.44% (21.76%), F 29.08% (29.51%).

1,3-*Dimethyl*-5-*trifluoromethyl*-4-*nitrosopyrazole*.—$\nu_{max}$(NaCl plate)/$cm^{-1}$ 1488, 1401, 1357, 1289, 1186, 1141, 1009, 779, 740; $\lambda_{max}(CH_2Cl_2)$/nm 716. *m*/*z* 193 [$M^+$, 100%].

**X-Ray crystallography.** Crystals of 3,5-di-*tert*-butyl-4-nitrosopyrazole (**2**) and 1,3,5-trimethyl-4-nitrosopyrazole (**3**) were obtained as described above and mounted on glass fibres using Araldite as adhesive. All crystallographic measurements were made using a FAST area detector diffractometer situated at the window of a rotating anode (Mo) generator operating at 50 kV, 55 mA ($\lambda$ = 0.710 69 Å) as previously described.[19] The crystal data and important parameters used for data collection and structure refinement are presented in Table 1. The unit cell parameters for each compound were determined by least-squares refinement of the diffractometer angles for 250 reflections.

The structures were solved by direct methods and refined on $F^2$ by full matrix least-squares using all unique data with intensities greater than zero. Both structures were found to be disordered, with different orientations of the NO group relative to the nitrogen substituent (H in **2** and Me in **3**). In **2**, the C(1)–N(1)/N(1′) and N(1)/N(1′)–O(1)/O(1′) distances were constrained to refine to the same values. In **3**, there are two molecules in the asymmetric unit, one without disorder and the other with disorder similar to that observed in **2**. All non-hydrogen atoms were anisotropic. The hydrogen atoms were included in calculated positions (riding model) with $U_{iso}$ tied to the $U_{eq}$ of the parent atom. The final *R* values are quoted in Table 1. The calculations were done on a Pentium P90 personal computer using the programs SHELXS86[20] (solution) and SHELXL93[21] (refinement). Absorption effects were ignored. Sources of scattering factor data are given in ref. 21.

Atomic coordinates, bond lengths and angles, and thermal parameters for **2** and **3** have been deposited at the Cambridge Crystallographic Data Centre (CCDC). For details of the deposition scheme, see 'Instructions for Authors', *J. Chem. Soc., Perkin Trans. 2*, 1997, Issue 1. Any request to the CCDC for this material should quote the full literature citation and the reference number 188/59.

## Results and discussion

### IR spectra

No IR data on 4-nitrosopyrazoles have been reported previously. This prompted an attempt to identify the wavenumbers of the NO stretching vibration in some of the compounds (*viz.* **1**–**4**, **9** and **10**). In view of the similar resonance interactions in 4-nitrosoanilines and 4-nitrosopyrazoles it is expected that the characteristic absorption of the nitroso group in these two types of compounds would be similar. Knieriem[22] has shown that in 4-nitrosoanilines the NO stretching vibration occurs as a strong absorption band in the range 1370–1330 $cm^{-1}$. All the 4-nitrosopyrazoles studied have strong absorptions in this region, these being absent in the spectra of un-nitrosated compounds. On that basis the following assignments of NO stretching modes were made: $\nu$/$cm^{-1}$ 1360 (**1**), 1343 (**2**), 1340 (**3**), 1352 (**4**), 1357 (**9**) and 1379 (**10**). These were all strong bands but no simple relationship with the nature of the ring substituent is evident.

### NMR spectra

The ambient temperature $^1H/^{19}F$ spectra of the compounds **1**–**10** were straightforwardly assigned (see Table 2), and were consistent with the N=O group rapidly rotating about its ring-attached N–C bond. On cooling, this rotation process was slowed, leading to considerable exchange broadening and eventual splitting of the signals of the 3- and 5-substituents. A similar but less pronounced effect was seen in the NMe signals of compounds **3**, **6**–**8** and **10**. These changes are clearly due to the separate detection of the individual rotamers of the R–N compounds (compounds **3**–**10**) and the single type of rotamer of

**Table 1** Crystal data and details of data collection and structure refinement for (**2**) and (**3**)

| | Compound (**2**) | Compound (**3**) |
|---|---|---|
| Empirical formula | $C_{11}H_{19}N_3O$ | $C_6H_9N_3O$ |
| Formula mass | 209.29 | 139.16 |
| $T$/K | 150(2) | 293(2) |
| Crystal system | Monoclinic | Orthorhombic |
| Space group | $P2_1/c$ (no. 14) | $Cmc2_1$ (no. 36) |
| $a$/Å | 10.7580(10) | 6.833(2) |
| $b$/Å | 9.7710(10) | 17.089(1) |
| $c$/Å | 12.2140 | 12.985(3) |
| $\alpha$/° | 90 | 90 |
| $\beta$/° | 109.844(5) | 90 |
| $\gamma$/° | 90 | 90 |
| $V$/Å$^{-3}$ | 1207.7(2) | 1516.2 |
| $Z$ | 4 | 8 |
| $D_c$/g cm$^{-3}$ | 1.151 | 1.219 |
| μ(Mo-Kα)/cm$^{-1}$ | 0.76 | 0.88 |
| $F$(000) | 456 | 592 |
| Crystal size/mm | 0.15 × 0.10 × 0.08 | 0.25 × 0.15 × 0.03 |
| $\theta$ range for data collection/degrees | 2.74 to 25.10 | 2.38 to 25.17 |
| $h_{min}$, $h_{max}$ | −12, 12 | −5, 7 |
| $k_{min}$, $k_{max}$ | −9, 11 | −18, 18 |
| $l_{min}$, $l_{max}$ | −13, 14 | −14, 14 |
| Reflections collected | 4475 | 2777 |
| Unique reflections | 1843 | 1115 |
| $R_{int}$ | 0.0624 | 0.0722 |
| Data/parameters in the refinement | 1843/166 | 1115/134 |
| Final $R$ [a] | $R_1$ = 0.0767 (0.0409) [b] | $R_1$ = 0.0832 (0.0425) |
| | $wR_2$ = 0.0899 (0.0845) [b] | $wR_2$ = 0.1095 (0.1002) |
| Largest diff. peak and hole/e Å$^{-3}$ | 0.142 and −0.132 | 0.105 and −0.077 |

[a] $R_1 = \Sigma(F_o - F_c)/\Sigma(F_o)$; $wR_2 = [\Sigma\{w(F_o^2 - F_c^2)^2\}/\Sigma\{w(F_o^2)^2\}]^{\frac{1}{2}}$; $w = 1/[\sigma^2(F_o^2) + (aP)^2]$ where $P = [\max(F_o^2) + 2F_c^2]/3$, and $a = 0.0266$ for (**2**) and 0.0568 for (**3**). [b] $R_1$ and $wR_2$ values for all unique data with intensities greater than zero; those calculated for data with $I > 2\sigma(I)$ are given in parentheses.

**Table 2** $^1$H/$^{19}$F NMR chemical shifts [a] of 4-nitrosopyrazoles at ambient and low temperatures

| | | | $\delta_H/\delta_F$ | | |
|---|---|---|---|---|---|
| Compound | $T$/K | Rotamer populations (%) | 1 | 3 | 5 |
| **1** | 303 | Average | — | 2.66 | 2.66 |
| | 228 | 100 [b] | | 2.25 [c] | 3.16 [d] |
| **2** | 303 | Average | — | 1.32 | 1.32 |
| | 193 | 100 [b] | — | 1.03 [c] | 1.62 [d] |
| **3** | 323 | Average | 3.77 | 2.37 | 2.81 |
| | 233 | 80 | 3.83 | 2.10 | 3.04 |
| | 233 | 20 | 3.71 | 2.94 | 2.23 |
| **4** | 303 | Average | 7.45–7.60 [e] | 2.43 | 2.92 |
| | 213 | 81 | ~7.5 [e] | 2.21 | 3.18 |
| | 213 | 19 | ~7.5 [e] | 3.08 | 2.28 |
| **5** | 303 | Average | 4.03 | 1.10 | 1.76 |
| | 163 | Average | 3.99 | 0.94 | 1.68 |
| **6** | 303 | Average | 3.84 | 7.5,[e] 8.2 [e] | 2.43 |
| | 213 | 88 | 3.85 | 7.6,[e] 8.2 [e] | 2.32 |
| | 213 | 12 | 3.98 | 7.5,[e] 8.2 [e] | 3.16 |
| **7** | 333 | Average | 3.79 | 2.36 | 1.04,[f] 2.20,[g] 3.14 [h] |
| | 228 | 86 | 3.86 | 2.13 | 1.05,[f] 2.26,[g] 3.37 [h] |
| | 228 | 14 | 3.73 | 2.98 | 0.86,[f] 1.60,[g] 2.30 [h] |
| **8** | 333 | Average | 3.80 | 0.95,[f] 1.98,[g] 2.71 [h] | 3.06 |
| | 233 | 75 | 3.86 | 0.83,[f] 1.60,[g] 2.31 [h] | 2.25 |
| | 233 | 25 | 3.75 | 1.01,[f] ?,[g] 3.32 [h] | 2.74 |
| **9** | 303 | Average | 4.06 [i] | 2.12 | 105.3 |
| | 263 | 99 | 4.05 [i] | 1.97 | 105.4 |
| | 263 | 1 | *j* | 3.01 | 102.4 |
| **10** | 303 | Average | 3.91 | 99.2 | 2.81 |
| | 183 | 85 | 3.91 | 97.2 | 3.14 |
| | 183 | 15 | 3.79 | 102.8 | 2.17 |

[a] $^1$H shifts rel. to $SiMe_4$ ($\delta = 0$); $^{19}$F shifts rel. to $C_6F_6$ ($\delta = 0$). [b] Single rotamers due to rapid NH tautomerism. [c] *syn* to −N=O. [d] *anti* to −N=O. [e] Multiplets. [f] $(CH_3)_2CH$−, $^3J_{HH}$ 6.6. [g] $(CH_3)_2CH$−$CH_2$−, $^3J_{HH}$ 6.6, 7.4. [h] $(CH_3)_2CH$−$CH_2$−, $J_{HH}$ 7.4. [i] $^5J_{HF}$ 1.3 Hz. [j] Signal too weak to be detected.

the H−N compounds (compounds **1**, **2**) where the two substituents, R′ and R″ are the same (Scheme 1).

The populations of the pairs of rotamers for the −N−R compounds are notably different in most cases (Table 2). Their assignments to *cis* and *trans* isomers was aided by low temperature NMR NOE difference experiments. The case of 1,3,5-trimethyl-4-nitrosopyrazole (**3**) will be described. Its low temperature solution spectrum is shown (Fig. 1). Irradiation of the 1-methyl signals of both isomers should lead to positive intensity enhancements of the spatially close 5-methyl signals. Such enhancements were detected in the higher frequency signal of the major rotamer and in the lower frequency signal of the

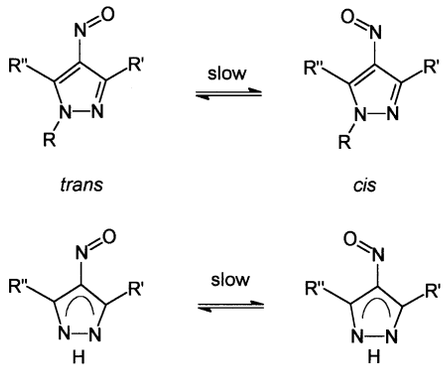


**Scheme 1**

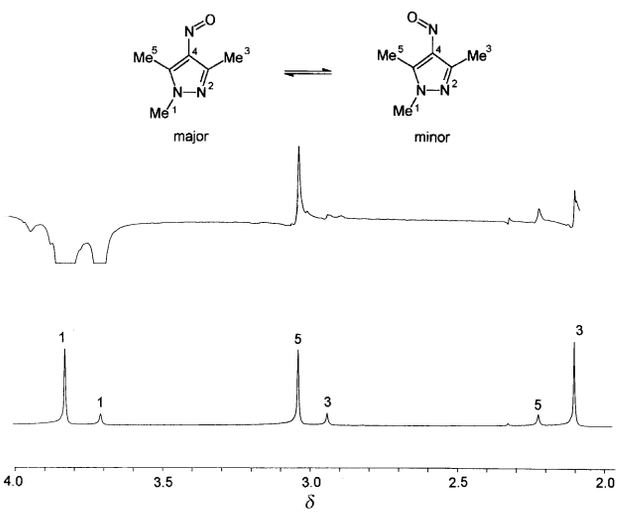


**Fig. 1** The 400 MHz $^1$H NMR NOE difference spectrum of 1,3,5-trimethyl-4-nitrosopyrazole (**3**) at 243 K in $CDCl_3$ showing the effect of irradiating the *N*-methyl signals of both rotamers

minor rotamer. It therefore appears that in the major rotamer the 5-methyl is deshielded and 3-methyl shielded. Assuming that the shielding anisotropy of the nitroso group in 4-nitrosopyrazoles is very similar to that of nitrosobenzenes,[4] the results imply that the nitroso group is pointing towards the 3-position of the ring in the major isomer, and towards the 5-position in the minor isomer. An X-ray crystallographic study (see below) confirmed that this was also the case in the solid state. It can therefore be concluded that when the 3- and 5-ring substituents are identical the −N=O group prefers to adopt a *trans* relationship with respect to the −N−R bond. *trans* Rotamers are also favoured when there are different alkyl substituents in the 3- and 5-positions, except in the 3-phenyl-5-methyl derivative (compound **6**) where the *cis*-rotamer is preferred, presumably as a result of the steric effects of the phenyl ring.

Points of interest arising from the NMR and X-ray crystallographic studies of individual compounds will now be discussed.

**3,5-Dimethyl-4-nitrosopyrazole (1).** On cooling a $CDCl_3$ solution of **1** the single methyl NMR signal broadened and then split into two equal intensity signals which were assigned to the methyl groups *syn* and *anti* with respect to the N=O group. The signals were sharp at 228 K indicating that at this temperature rapid tautomeric exchange of the hydrogen between the two ring nitrogens was occurring. The changes in bandshape of the methyl signals with temperature were computed using the DNMR3 program and 'best-fit' rate constants obtained.

**3,5-Di-*tert*-butyl-4-nitrosopyrazole (2).** A solution of **2** in $CD_2Cl_2$ was cooled to 193 K, during which time the *tert*-butyl signal broadened, then split into two equal intensity signals, and then continued to broaden. These bandshape changes could not be fitted in terms of a simple two-site exchange associated with

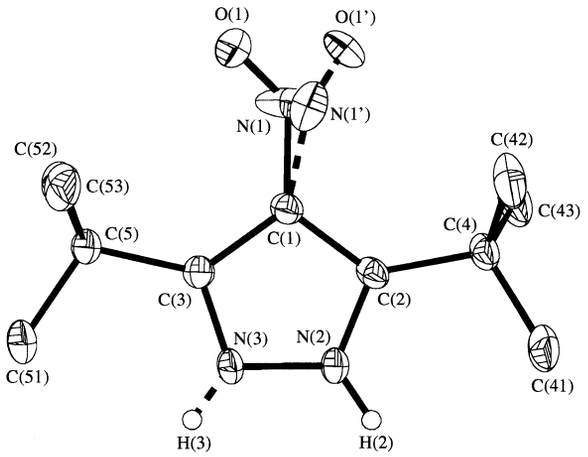


**Fig. 2** A view of the crystal structure of 1-*H*-3,5-di-*tert*-butyl-4-nitrosopyrazole (**2**) giving the atom labelling for both structures. (Broken bonds refer to minor form.)

the restricted rotation of the nitroso group. The spectral changes implied that a second rate process was also being detected. Since studies on 1-methyl-3,5-di-*tert*-butyl-4-nitrosopyrazole (**5**) (see later) showed that N=O rotation was still rapid at 193 K when flanking *tert*-butyl groups are present, the bandshape changes in **2** were attributed primarily to a slowing down of the tautomeric exchange. Since traces of acid are known to increase the rate of NH exchange, a small quantity of ethanoic acid was added to a $CDCl_3$ solution of **2**, and to a $CDCl_3$ solution of 3,5-dimethyl-4-nitrosopyrazole (**1**). The effect on the variable temperature spectra of **2** was to significantly increase the exchange rates leading to coalescence of the signals at a temperature *ca.* 10 K lower than previously. In contrast, the effect on the spectra of **1** was insignificant. These observations confirm that the lineshape changes observed in **1** are due to restricted NO rotation (which will be largely unaffected by the presence of acid) whereas the changes in **2** are due to a combination of tautomeric exchange and NO rotation (Scheme 2).

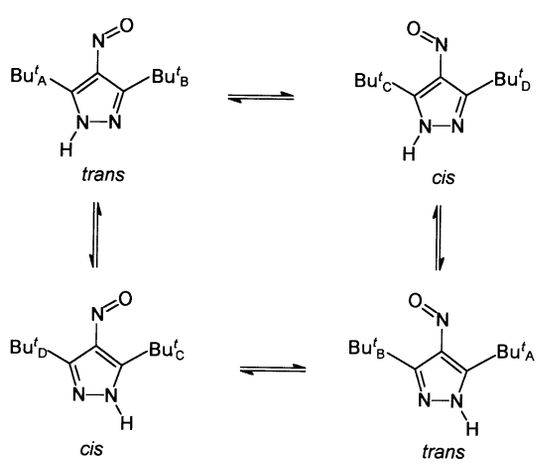


**Scheme 2**

Unfortunately, it was not possible to cool the solution sufficiently to obtain the spectra of the non-exchanging *cis* and *trans* species, so no rate data could be extracted.

**Crystal structure of (2).** A view of the crystal structure of **2** measured at 150 K is shown in Fig. 2. The structure is disordered and can be formulated as a 67/33% mixture of structures each with the −N=O group *trans* to the −N−H bond. In each form the −N=O group is twisted slightly out of the $C_3N_2$ ring plane. Deviations (Å) of the nitroso group atoms from the ring plane are −0.139 [N(1)] and 0.095 [O(1)] for the more abundant form and 0.220 [(N1′)] and −0.344 [O(1′)] for the less abundant form. This twisting of the −N=O group from

**Table 3** $^{13}$C CP/MAS shift data, $\delta_c$, for 1,3,5-trimethyl-4-nitrosopyrazole (**3**) at 303 K

| | Ring carbons[a] | | | Methyl carbons[a] | | |
|---|---|---|---|---|---|---|
| Isomer | 3/3′ | 4/4′ | 5/5′ | 1/1′ | 3/3′ | 5/5′ |
| Major | 133.3 | 160.4 | 151.5 | 35.4 | 14.0 | 9.6 |
| Minor | 154.5 | 160.4 | 125.3 | ~35 | ~13 | ~11 |

[a] Unprimed values refer to major rotamer (see Fig. 3).

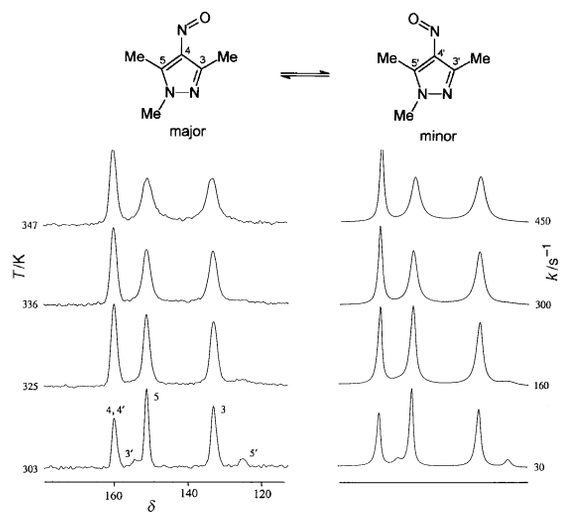


**Fig. 3** Variable temperature $^{13}$C CP/MAS NMR spectra of 1,3,5-trimethyl-4-nitrosopyrazole (**3**) showing the effects of restricted N=O rotation. 'Best-fit' rate constants for the computed spectra (right) are indicated.

coplanarity with the ring could account for the rotation barrier being too low to be measured by NMR since the twist from coplanarity will reduce the energy difference between the ground and transition state structure in which the −N=O group will be approximately orthogonal with respect to the ring. The bond lengths and angles associated with the −N=O groups are unusual. The N=O bond lengths are 1.053(10) Å (major) and 1.048(11) Å (minor), the C–N bond lengths are 1.394(3) Å (major) and 1.391(4) Å (minor) and the CNO angles are 130.7(11)° (major) and 134.1(13)° (minor). These N=O bond lengths are exceptionally short and the CNO bond angles are exceptionally wide when compared to data for *C*-nitrosobenzenes and 1,3,5-trimethyl-4-nitrosopyrazole (**3**) (see later). A fuller discussion of these data will be given in the next section.

**1,3,5-Trimethyl-4-nitrosopyrazole (3).** Low temperature $^{1}$H NMR solution studies showed the changes expected for restricted rotation of the −N=O group. The three signals at room temperature broadened on cooling and eventually split into unequal intensity pairs of signals due to the *cis* and *trans* rotamers, as depicted in Fig. 1. Bandshape analysis of all the methyl signals yielded accurate kinetic data for the rotation process. In earlier work on *p*-nitrosoanilines[4] we established that the nitroso group rotates relatively freely in the solid state. We therefore sought detection of the same phenomenon in nitrosopyrazoles. Accordingly, the $^{13}$C NMR CP/MAS spectra of solid **3** were recorded at ambient temperatures (Fig. 3). The room temperature spectrum consists of three strong ring carbon signals and three strong methyl signals plus a weaker set of signals of both functional types. Clearly, the two sets are due to the *cis*- and *trans*-rotamers (Scheme 1) and signal assignments (Table 3), were aided by comparison with the $^{13}$C solution-state data[1] and a solution-state $^{1}$H–$^{13}$C HMQC COSY spectrum. On heating the solid spectral changes occurred which were fully consistent with the onset of rotation of the −N=O group. This was seen most clearly in the ring carbon region of the spectrum where exchange occurs between the 3- and 3′-carbons and between the 5- and 5′-carbons (Fig. 3). The band due to the 4-position carbon in both isomers (*viz.* C4 and C4′) did not change significantly due to the near-isochronous nature of these carbons. Bandshape analysis was performed on the ring carbon spectrum at four temperatures between 303 and 347 K, and approximate 'best-fit' rate data deduced (Fig. 3).

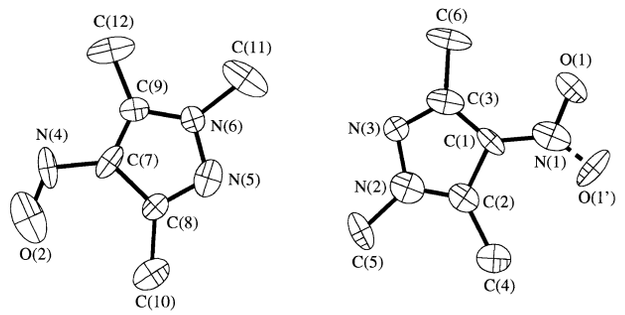


**Fig. 4** The two independent molecules of 1,3,5-trimethyl-4-nitrosopyrazole (**3**) in the unit cell. The minor *cis*-form is indicated by the broken N(1)–O(1′) bond.

**Crystal structure of (3).** The crystal structure of **3** (Fig. 4) revealed that there are two independent molecules in the unit cell, both on the minor plane (at $x = 0$) and related by a non-crystallographic two-fold axis. One molecule is clearly *trans* and the other is 84% *trans* and 16% *cis*. Thus, overall the sample from which the X-ray data were obtained constitutes 92% *trans* and 8% *cis* forms. This result is consistent with the solution and solid-state NMR studies where the *trans*/*cis* ratios were *ca.* 80/20% in solution at 233 K and in the solid at ambient temperatures. The unit cell, Fig. 5(*a*), consists of two molecules of the *trans* form and two molecules of the *trans–cis* form. There was no evidence in the solid state CP/MAS spectrum of distinction between the two molecules of either form, presumably due to insufficient $^{13}$C chemical shift differences. The molecules are packed in layers [Fig. 5(*b*)] with a relatively large interlayer separation of *ca.* 3.4 Å. Unfortunately, this meant that structural data could only be obtained at room temperature as at low temperatures the crystals cracked. In the *trans* molecule the bond lengths and angles of the nitroso group are very similar to those found in substituted nitrosobenzenes which possess strong intramolecular resonance interactions. Thus, the values $r_{NO} = 1.209(6)$, $r_{CN} = 1.401(12)$ Å and ∠CNO = 116.5(10)° should be compared with values for $r_{NO} = 1.227$–$1.27$,[23,24] $r_{CN} = 1.340$–$1.467$ Å[23–29] and ∠CNO = 112.7–117.2°[23–29] found in 4-nitroso-anilines and -phenolates. The *cis* form differs remarkably from the *trans* form in its CNO angle. This has now opened up to 138(2)° compared to 117.1(9)° in the *trans* form. It is uncertain whether this is a real effect or whether it results from disorder.

A comparison of the crystal data of the *trans* form of **3** with that of **2** where the −N=O group has flanking *tert*-butyl groups reveals considerable differences. N=O bond lengths in **2** are abnormally short and CNO angles are remarkably large. This may be associated with the considerable twist of the nitroso group out of the ring plane, whereas in **3** the N=O group is virtually coplanar with the ring (Fig. 5). This difference probably accounts for the rotation energy barrier in **3** being considerably higher than in **2** where the ground state structure is closer (in geometry and energy) to the orthogonal transition state structure.

**1-Phenyl-3,5-dimethyl-4-nitrosopyrazole (4).** This compound exhibited very similar low temperature solution NMR properties to **3**, indicating that the rotational characteristics of the −N=O group are little affected by the substituent attached to the pyrazole nitrogen, N(1).

**1-Methyl-3,5-di-*tert*-butyl-4-nitrosopyrazole (5).** On cooling to *ca.* 173 K in $CD_2Cl_2$ no significant changes were detected in

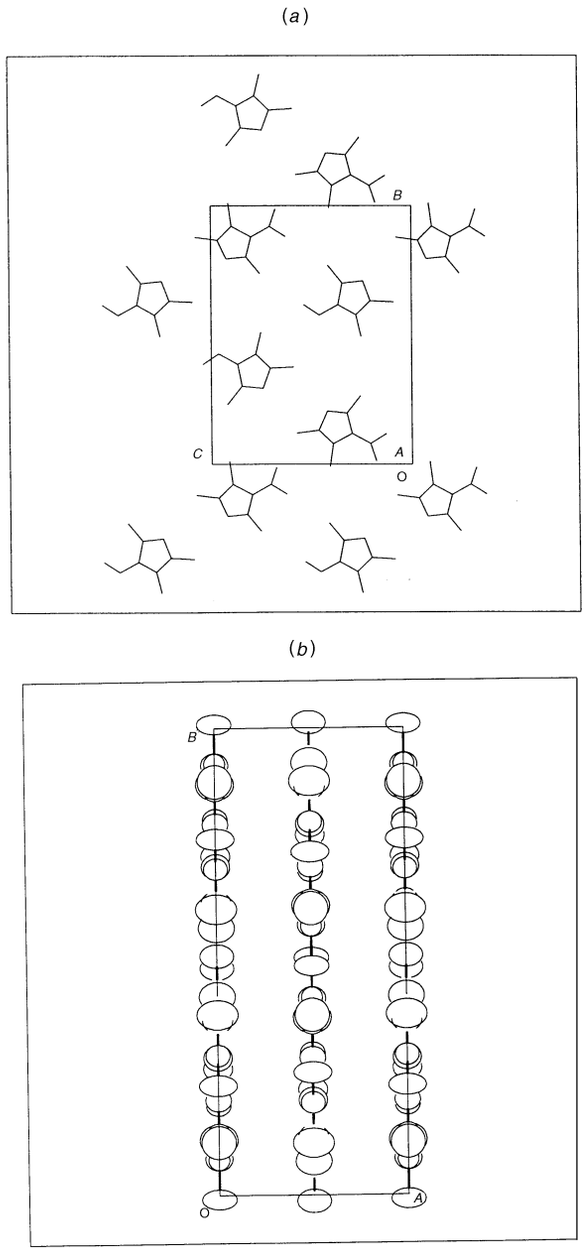


**Fig. 5** The crystal packing of 1,3,5-trimethyl-4-nitrosopyrazole (**3**), (*a*) viewed on the *bc* plane, all molecules at height 280, (*b*) viewed along *c*, interlayer separation being 3.42 Å

the *tert*-butyl and 1-methyl signals. This clearly indicated that the −N=O group rotation was still rapid on the $^1$H NMR time-scale even at this low temperature. This was attributed to the flanking *tert*-butyl groups in the ground state structure forcing the −N=O group towards the orthogonal transition state structure thus lowering the energy barrier (*cf.* compound **2** also).

**1,5-Dimethyl-3-phenyl-4-nitrosopyrazole (6).** A solution of **6** in $CDCl_3$ was cooled to 213 K and the expected changes in the 1- and 5-methyl signals were observed. These bandshapes were fitted in the usual way using the DNMR3 program[14] and accurate rate data obtained. This compound was unusual in that the major rotational isomer was the *cis*-isomer as a result of the steric requirements of the 3-phenyl substituent.

**1,3-Dimethyl-5-isobutyl-4-nitrosopyrazole (7).** On cooling this compound the cessation of rotation of the −N=O group was seen by large splittings of the 3-methyl signal and the $-CH_2-$signal of the isobutyl group, together with smaller splittings of the 1-methyl signal and the −CH− and $CH_3$ signals of the isobutyl group. Bandshape fittings on the 3-methyl signal yielded rate data for the nitroso group notation.

**Table 4** Activation energy parameters for nitroso-group rotation in substituted 4-nitrosopyrazoles

| Compound | Rotamers | $\Delta H^{\ddagger}$/ kJ mol$^{-1}$ | $\Delta S^{\ddagger}$/ J K$^{-1}$ mol$^{-1}$ | $\Delta G^{\ddagger a}$/ kJ mol$^{-1}$ |
|---|---|---|---|---|
| **1** | | 70.9 ± 1.0 | 67 ± 4 | 50.8 ± 0.1 |
| **3** | major ⟶ minor | 62.7 ± 1.4 | 23 ± 5 | 55.8 ± 0.7 |
| | minor ⟶ major | 59.7 ± 0.9 | 23 ± 5 | 52.8 ± 0.7 |
| **3** | major ⟶ minor[b] | *ca.* 52 | *ca.* −44 | *ca.* 65 |
| | minor ⟶ major[b] | *ca.* 49 | *ca.* −44 | *ca.* 62 |
| **4** | major ⟶ minor | 72.9 ± 0.7 | 70 ± 3 | 51.9 ± 0.1 |
| | minor ⟶ major | 70.0 ± 0.7 | 70 ± 3 | 49.0 ± 0.1 |
| **6** | major ⟶ minor[c] | 63.7 ± 0.5 | 50 ± 1 | 48.7 ± 0.1 |
| | minor ⟶ major[c] | 60.2 ± 0.5 | 50 ± 1 | 45.2 ± 0.1 |
| **7** | major ⟶ minor | 66.4 ± 1.1 | 40 ± 4 | 54.6 ± 0.1 |
| | minor ⟶ major | 63.4 ± 1.1 | 40 ± 4 | 51.6 ± 0.1 |
| **8** | major ⟶ minor | 64.3 ± 0.4 | 34 ± 2 | 54.0 ± 0.1 |
| | minor ⟶ major | 62.3 ± 0.4 | 34 ± 2 | 52.0 ± 0.1 |
| **9** | major ⟶ minor | 43.3 ± 0.5 | 17 ± 2 | 38.2 ± 0.3 |
| | minor ⟶ major | 37.1 ± 0.5 | 17 ± 2 | 32.0 ± 0.3 |
| **10** | major ⟶ minor | 48.0 ± 0.6 | 13 ± 2 | 44.3 ± 0.2 |
| | minor ⟶ major | 45.8 ± 0.6 | 13 ± 2 | 42.1 ± 0.2 |

[a] At 298.14 K. [b] Solid-state NMR data. [c] *cis*-Form is favoured; in all other cases *trans* is dominant.

**1,5-Dimethyl-3-isobutyl-4-nitrosopyrazole (8).** This structural isomer of **7** exhibited very analogous NMR properties. Bandshape analysis was applied to the 5-methyl signals as these changed most on cooling. It is noteworthy that the rotamer populations were somewhat less dissimilar (75/25%) in **8** than in **7** where they were 86/14%. In compound **7** the preferred *trans* rotamer involves the N=O group directed towards the methyl group, whereas in **8** it is directed towards the bulkier isobutyl substituent.

**1,3-Dimethyl-5-trifluoromethyl-4-nitrosopyrazole (9).** The different steric effects of flanking groups to the nitroso group is seen vividly in this compound, as compared to its structural isomer **10** (see later). In **9** the *trans* structure places the N=O pointing towards the less bulky methyl group (compared to $CF_3$) causing this structure to be overwhelmingly favoured (*ca.* 99%). The large intensity imbalance of the signals of the *trans* and *cis* forms made bandshape analysis difficult, but satisfactory fittings were achieved on the $^{19}$F signals of the $CF_3$ group. This sharp signal at ambient temperature broadened considerably on cooling and eventually split into two signals, the minor one being detected with difficulty at temperatures below 178 K.

**1-5-Dimethyl-3-trifluoromethyl-4-nitrosopyrazole (10).** In this structural isomer of **9** the N=O group in the *trans* rotamer points towards the $CF_3$ group. This is a less favourable situation than in **9** and it causes the population of this rotamer to be depressed (compared to **9**) so that the new *trans*/*cis* population ratio is 85/15%. $^1$H NMR spectra of the 5-methyl signals of **10** in the temperature range 188–263 K are shown in Fig. 6. Bandshape analysis produced very satisfactory computer fits which led to reliable rate data for the nitroso group rotation.

**Nitroso group rotational energy barriers.** Activation parameters for the N=O rotation process were able to be calculated for all compounds except **2** and **5**. These are collected in Table 4. $\Delta G^{\ddagger}$ (298 K) values are least prone to systematic error and so energy barriers will be discussed in terms of this parameter. $\Delta H^{\ddagger}$ values are consistently higher than the corresponding $\Delta G^{\ddagger}$ values as a result of positive $\Delta S^{\ddagger}$ values (except in the solid state $^{13}$C study). Activation entropies are most difficult to measure accurately but the consistency of their magnitudes and signs in Table 4 suggests that they are reliably measured here and point to an orthogonal transition state structure which has rather more motional degrees of freedom compared to the ground state structures.

Magnitudes of $\Delta G^{\ddagger}$ for compounds **1**–**8** fall in the range 45–56 kJ mol$^{-1}$ for solution studies. These magnitudes are similar to those for *p*-nitrosoanilines[4] showing that the C−NO bond

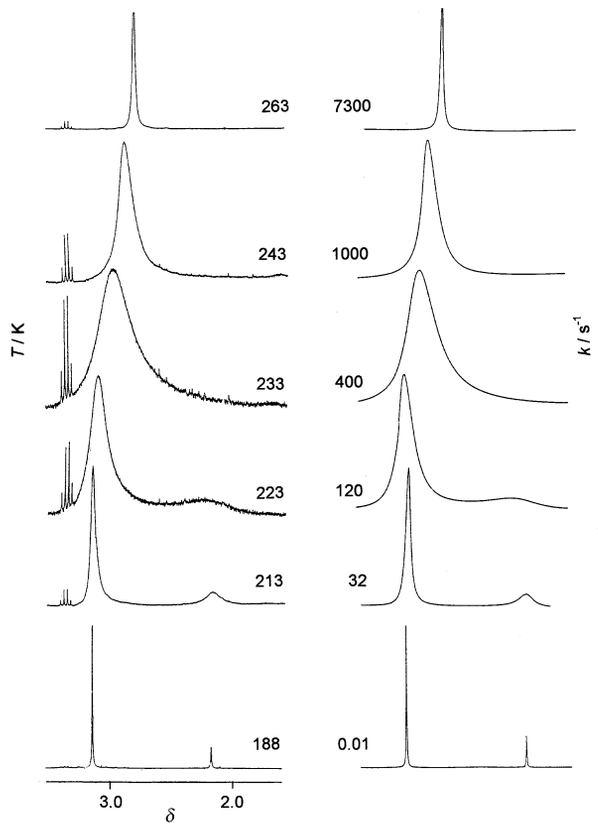


**Fig. 6** The 300 MHz variable temperature $^1$H NMR spectra of 1,5-dimethyl-3-trifluoromethyl-4-nitrosopyrazole (**10**) in $CD_2Cl_2$ showing the effects of varying rates of −N=O rotation on the 5-methyl signals. Theoretical spectra with 'best-fit' rate constants are shown alongside.

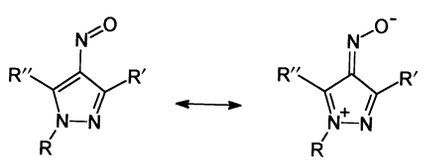

**Scheme 3**

has significant double bond character arising from canonical forms (Scheme 3). These rotational barriers are especially high in view of the steric interactions that will arise from the flanking alkyl/aryl groups. Steric effects in 4-nitrosoanilines reduced the barriers to rotation by *ca.* 15 kJ mol$^{-1}$,[4] due to the raising of the ground state energies of these compounds. The effects of the flanking alkyl/aryl groups in 4-nitrosopyrazoles will be less significant since the groups attached to a five-membered ring will be directed further away from the nitroso group than for a six-membered ring derivative.

For compound **3** the data show that the N=O rotation in the solid state is somewhat more restricted than in the dissolved state, with the energy barrier ($\Delta G^{\ddagger}$) being *ca.* 10 kJ mol$^{-1}$ higher. The $\Delta S^{\ddagger}$ value for the solid state study is negative as it is for *p*-dimethylaminonitrosobenzene in the solid state.[4] It is uncertain whether this is a genuine feature of the rotation process in the solid state or whether it is due to systematic errors in fitting the solid state spectral line shapes.

The energy difference between the ground states of the pairs of rotamers for the 1-substituted nitrosopyrazoles is *ca.* 3 kJ mol$^{-1}$, and this also applies to the solid state. This energy corresponds to an approximate population ratio for the two rotameric forms of 80/20% in favour of the *trans* form. This is a surprisingly large population imbalance. It may primarily be the result of the zig–zag relationship between the N=O and the C(4)=C(5) double bond which leads to more effective π-electron delocalisation in the *trans* form compared to the *cis*-form.

The N=O rotational energy barriers are significantly lower for compounds **9** and **10** where a flanking $CF_3$ group is present. This is probably the result of the electron withdrawing nature of the $CF_3$ group, which will remove electron density from the ring and also reduce the double bond character of the C–NO bond. The relative steric effects of $CF_3$ and $CH_3$ groups should also be considered. Clearly, the $CF_3$ group produces a greater steric restraint on the −N=O group than does a $CH_3$ group. This is reflected in the large difference in rotamer populations for these two structural isomers. The N=O group is clearly much stabilised when it is directed towards a flanking $CH_3$ rather than a $CF_3$ group. In addition to steric factors, hyperconjugation may also play a stabilising role in this geometry.

It is noteworthy that there was no evidence in the NMR spectra of any of these nitrosopyrazoles, even at the lowest attainable temperatures, of any azodioxy dimer formation which is a common feature of many *C*-nitrosobenzenes[30] and *C*-nitrosoalkanes.[31] However, we have shown earlier[30] that dimer formation of *C*-nitroso compounds will be expected only if they exhibit NO stretching modes in the range 1590–1480 cm$^{-1}$. The present nitrosopyrazoles exhibit values in the range 1379–1340 cm$^{-1}$, which are similar in magnitude to those of nitrosoanilines, which similarly do not show any dimerisation tendencies. The present results are thus fully consistent with previous findings.

## Acknowledgements

We are most grateful to the University of Exeter for the award of a Frank Southerden scholarship (to D. A. F.). We wish to thank the EPSRC for use of the solid state NMR service at the University of Durham Industrial Research Laboratories, and for the X-ray crystallography service at the University of Wales, Cardiff.

## References

1 Part 1, M. Cameron, B. G. Gowenlock and A. S. F. Boyd, *J. Chem. Soc., Perkin Trans. 2*, 1996, 2271.
2 L. Wolff, P. Bock, G. Lorentz and P. Trappe, *Liebigs Ann. Chem.*, 1902, **325**, 129.
3 J. Sandstrom, *Dynamic NMR Spectroscopy*, Academic, London, 1982.
4 D. A. Fletcher, B. G. Gowenlock, K. G. Orrell and V. Šik, *Magn. Reson. Chem.*, 1995, **33**, 561, and references therein.
5 M. D. Lumsden, G. Wu, R. E. Wasylishen and R. D. Curtis, *J. Am. Chem. Soc.*, 1993, **115**, 2825.
6 D. A. Fletcher, Ph.D. Thesis, University of Exeter, 1996.
7 G. L. McNew and N. K. Sundholm, *Phytopathology*, 1949, **39**, 721.
8 S. E. Torf, N. I. Kudryashova, N. V. Khromov-Bonner and T. A. Mikhailova, *J. Gen. Chem.* (*USSR*), 1962, **32**, 1726.
9 G. V. Boyd and T. Norris, *J. Chem. Soc., Perkin Trans. 1*, 1974, 1028.
10 R. Hüttel, F. Büchele and P. Jochum, *Chem. Ber.*, 1955, **88**, 1577.
11 C. L. Habraken, C. I. M. Beenakker and J. Brusee, *J. Heterocycl. Chem.*, 1972, **9**, 939.
12 G. A. Lanovaya, V. P. Micheeva and S. V. Orlova, *Khim. Geterotskii. Soed.*, 1989, **25**, 337.
13 F. Aguilar-Parilla, C. Cativiela, M. D. D. de Villegas, J. Elguero, C. Foces-Foces, J. I. G. Laureiro, F. H. Cano, H.-H. Limbach, J. A. S. Smith and C. Toiron, *J. Chem. Soc., Perkin Trans. 2*, 1992, 1737, and references therein.
14 G. Binsch and D. A. Kleier, Program 165, Quantum Chemistry Program Exchange, Indiana University, IN, 1970.
15 V. Šik, Ph.D. Thesis, University of Exeter, 1979.
16 E. W. Abel, T. P. J. Coston, K. G. Orrell, V. Šik and D. Stephenson, *J. Magn. Reson.*, 1986, **70**, 34.
17 S. J. Opella and M. H. Frey, *J. Am. Chem. Soc.*, 1979, **101**, 5854.
18 W. T. Dixon, *J. Chem. Phys.*, 1982, **77**, 1800.
19 J. A. Darr, S. R. Drake, M. B. Hursthouse and K. M. A. Malik, *Inorg. Chem.*, 1993, **32**, 5104.
20 G. M. Sheldrick, *Acta Crystallogr. Sect. A*, 1990, **46**, 467.
21 G. M. Sheldrick, SHELXL-93, Program for Crystal Structure Refinement, University of Göttingen, 1993.
22 B. Knieriem, Doctoral thesis, University of Göttingen, 1972.
23 H. J. Talberg, *Acta Chem. Scand., Ser. A*, 1977, **31**, 743.

24 R. Dunlop, A. D. U. Hardy, H. H. Mills, R. K. Mackenzie, D. D. MacNicol and D. A. R. Williams, *J. Chem. Res., (S)*, 1979, 152; *J. Chem. Res. (M)*, 1979, 1848.
25 H. J. Talberg, *Acta Chem. Scand., Ser. A*, 1979, **33**, 289.
26 H. J. Talberg, *Acta Chem. Scand., Ser. A*, 1977, **31**, 485.
27 H. J. Talberg, *Acta Chem. Scand., Ser. A*, 1976, **30**, 829.
28 H. J. Talberg, *Acta Chem. Scand., Ser. A*, 1977, **31**, 37.
29 H. J. Talberg, *Acta Chem. Scand., Ser. A*, 1975, **29**, 919.
30 D. A. Fletcher, B. G. Gowenlock, K. G. Orrell, V. Šik, D. E. Hibbs, M. B. Hursthouse and K. M. A. Malik, *J. Chem. Soc., Perkin Trans. 2*, 1996, 191.
31 R. Glaser, R. K. Murmann and C. L. Barnes, *J. Org. Chem.*, 1996, **61**, 1047.

*Paper* 6/07063I
*Received* 16*th October* 1996
*Accepted* 5*th December* 1996